RSC Advances

ROYAL SOCIETY OF CHEMISTRY

www.rsc.org/advances

Journal Name

ARTICLE

DNA hybridization on silicon nanowire platform prepared by glancing angle deposition and metal assisted chemical etching process

Received 00th January 20xx,
Accepted 00th January 20xx

DOI: 10.1039/x0xx00000x

www.rsc.org/

H. Cheng,[a] J. X. Wu,[b] H. Zheng,[c] W. Xu,[d] L. Zhou,[e] H. P. Too[f,g] and W. K. Choi†[a,b,d]

Silicon nanowire platform prepared by glancing angle depositionn and nmetal assisted chemiocal etching (GLAD-MACE) was used for oligonucleotides hybridization. The limit of detection of this platform was enhanced due to the huge amount of probe molecules that can be accommodated on the nanowires surface and pores on the sidewall. In contrast to conventional substrate, the GLAD-MACE nanowires can accept 100 times more probes without showing probe steric hindrance. Compared to detection of oligonucleotides with fluorescent reporters on a traditional substrate, even those with the facilitate of microfluidic mixing chamber, at least a 10 times lower LoD can be reached with a passive hybridization strategy. For device built with GLAD-MACE nanowires, it is clear that one important factor to optimize the system performance is to design an apparatus that can speed up the diffusion process of antisenses.

1. Introduction

Oligonucleotide arrays, or analyte specific arrays in general, have attracted great attentions due to their ability to perform simultaneous high throughput screenings of multiple analytes. However, this technology also faces challenges as compared to, say, quantitative real-time Polymerase Chain Reaction (qPCR) due to its lower sensitivity and specificity of detection.[1,2] This could be due problems such as surface-probe interaction and the lack of chain reaction amplification.

Bio-analytic applications ideally require high signal to noise ratios (SNRs). One solution is to increase the amount of probe loaded on the array surface[3-5] such that a larger amount of targets can be captured. However, overcrowded probe immobilization leads to a reduction of target capturing due to steric hindrance.[6] Researchers have sought to produce structured surfaces to increase surface area (in order to decrease the actual density of immobilized molecules) such that the steric hindrance can be reduced.[7] For example, polymers such as Poly(amidoamine) (PAMAM) have been coated on glass slide surface[8] to form nano-scale (3-5 nm) topographical structures, and micro- and nano-structures based substrates were developed to enhance biomolecules interaction or immobilization.[9] For example, by immobilization glucose oxidase into porous materials, the enzymatic activities per substrate increased over 100 folds compared to flat substrates.[10] For microarray, Murthy *et al*.[11] have shown that by using nanopillar arrays the signal readout increased 7 times compared to flat silicon wafer. Other researchers[12,13] have developed similar platform on plastic to enhance the capturing of DNA targets.

In our previous work, we have shown that the nanowires prepared by the glancing angle deposition-metal assisted chemical etching (GLAD-MACE) method exhibited high surface loading capacity which can be used for increasing the detection sensitivity.[14] However, accurate characterization of GLAD-MACE nanowires for oligonucleotide immobilization and hybridization is difficult. Conventional method for surface quantification that involves the use of Brunauer–Emmett–Teller (BET) approach is not suitable as it requires large amount of samples and also uses gas molecules that are not comparable to biomolecules in terms of size. Fluorescent scanning, despite being a fast in-situ characterization approach, lacks the quantitative precision that correlates fluorescent unit to the absolute amount of molecules present. In addition, fluorescent scanning is often confounded by uncertainties such as fluorescent quenching as well as energy transfer. Due to the 3D topographical structures and the insulating oxide on the surface of the GLAD-MACE nanowires, method such as surface plasmon resonance (SPR) is hard to apply and calibration. In this paper, GLAD-MACE substrate is characterized with fluorometry method with fluorophore linked oligonucleotides. We showed quantitatively that GLAD-MACE substrate can accommodate oligonucleotides with concentration 2 orders of magnitudes higher than that reported with

[a] *Advanced Materials for Micro- and Nano- Systems, Singapore-MIT Alliance, Singapore 117583*
[b] *NUS Graduate School for Integrative Sciences and Engineering, National University of Singapore, Singapore 117456*
[c] *GLOBALFOUNDRIES Singapore Pte. Ltd, Singapore 738406*
[d] *Department of Electrical and Computer Engineering, National University of Singapore, Singapore 117583*
[e] *MiREXS Pte Ltd., 10 Biopolis Road, #03-01 Chromos, Singapore 138670*
[f] *Department of Biochemistry, National University of Singapore, Singapore 117597*
[g] *Bioprocessing Technology Institute, 20 Biopolis Way, #06-01 Centros, Singapore 138668*
† H. Cheng and J.X. Wu contributed equally to experiments performed in this work.
Email: elechoi@nus.edu.sg; Tel: 65-6515 6473
Electronic Supplementary Information (ESI) available: See
DOI: 10.1039/x0xx00000x

conventional substrate. Furthermore, we demonstrated that steric hindrance effect, which can be observed on substrate with high concentration of oligonucleotide functionalization, is absent on GLAD-MACE substrate. We further analysed important factors influencing the performance of GLAD-MACE substrate with both static and dynamic cases.

2. Experimental

Materials and Methods

Substrate fabrication

To fabricate GLAD-MACE substrate, cleaned Si wafer was placed in an e-beam evaporator at vacuum below 10^{-6} torr; and evaporation pressure was around 10^{-5} torr during evaporation. Au evaporation was performed with an oblique angle of 87 degrees to the surface normal of the substrate. The substrate was slowly rotated at 0.2 rpm to ensure a symmetrical deposition of the incoming atoms. After deposition, Au clusters will form on the substrate. The wafer was then etched in a solution composed of H_2O, HF (4.6 M) and H_2O_2 (0.44M) at room temperature. Finally, Au on the Si surface was removed using a standard gold etchant and the nanostructured substrate was oxidized in O_2 at 900^0C for 35 min. The resultant silicon nanowires are of diameters ranging from 10 nm to 100 nm. In this work, we produced nanowires with height around 10 μm with detailed description of the nanowire platform shown in Supplementary S1.

Crosslinking of oligonucleotides

GLAD-MACE nanowires and porous silica beads (from Fuji Silysia Chemical Ltd) were silanized and functionalized with adipic acid to graft a carboxyl group on the surface. The adipic acid was dissolved in 0.1 M MES buffer with pH = 6 to avoid precipitation in subsequent steps. The final concentration of adipic acid in MES buffer was 1.3%. The solution was aliquoted and stored in 4^0C before use. 1-Ethyl-3-[3-dimethylaminopropyl]carbodiimide hydrochloride (EDC·HCl) was used to crosslink adipic acid with APTES. EDC powder was dissolved in 0.1M MES buffer at pH 6, aliquoted and stored immediately in -20^0C.

The silanized GLAD-MACE nanowire substrates were carboxylated with 1% adipic acid and 0.25M EDC for 2 hours at room temperature and washed with 1M Tris buffer at pH 8 for 10 minutes, and then 0.1 M MES buffer at pH 6 for 10 minutes before finally rinsed with water and dried with absolute ethanol.

Aminated (5' end with a 6 carbon linker) oligonucleotides were purchased from Sigma-Aldrich, Integrated DNA Technologies (IDT) or AITbiotech with standard desalting purification for oligonucleotides without fluorescent dye conjugation. For oligonucleotides conjugated with dye, high performance liquid chromatography (HPLC) purification was used. Oligonucleotides The dissolved oligonucleotides were stored in -20^0C before use.

To crosslink aminated oligonucleotides to carboxylated nanowires, a mixed solution containing oligonucleotides at desired concentration, 0.25 M EDC and 0.1M MES at pH 6 was used. The solution was dropped on top of the nanowires and incubated for desired time inside a humid chamber to prevent the solution from drying. After incubation, the substrate were washed with 1M Tris buffer at pH 8.5 for 10 minutes to terminate the reaction, and then washed with a 1%-2% SDS solution in 4X PBS buffer (548 mM NaCl, 10.8 mM KCl, 40 mM Na_2HPO_4 and 8 mM KH_2PO_4) heated above 60^0C for 20 minutes to remove any oligonucleotides that were not covalently linked to the nanowires. Finally, the GLAD-MACE substrate was washed with 0.1M MES buffer for 10 minutes and dried with pure ethanol. Note that oligonucleotides functionalized on nanowires were refereed as sense strand in this paper.

Hybridization of oligonucleotides

Hybridization of matched or mismatched oligonucleotides (hereafter referred as antisenses) was performed in PBS buffer or Tris-Acetate-Ethylenediaminetetraacetic acid (EDTA) (TAE) buffer of various salt concentrations and temperatures. Typically, Triton X100 (TX100) was added in the hybridization solution to a concentration of 2%, so that error in hybridization/nonspecific binding to substrate will be reduced. After hybridization, substrates were washed with 2% TX100 in PBS for 3 times, 10 minutes each time. The substrates were then spin dried with by centrifuge at 500×g for 5 minutes, or ethanol dried.

To estimate equilibrium constant of hybridization, the concentration of oligonucleotide covalently bound to surface as well as un-hybridized remaining antisense concentration had to measured. To measure the crosslinked sense oligonucleotides, known amount of fluorophore conjugated oligonucleotide with amine modification was incubated to react with carboxylated nanowire. After reaction, the substrates were washed with washing buffer thoroughly. 30 μL of washing solution was measured in Greiner Bio 384 well plate to determine the concentration of unreacted oligonucleotides, with the volume of total washing solution known, the amount of unreacted oligonucleotides can be gauged.

To measure the equilibrium constant, known amount of oligonucleotides were dissolved in hybridization buffer; and hybridization was proceeded until equilibrium. To ensure equilibrium has been reached, the substrates were placed into a lab assembled stirring machine for 152 hours at room temperature. The stirring speed was set to 70 rpm and the reaction volume was at 320 μL. According to Buchegger *et al*.,[15] the shear flow induced by the stirring machine will break the diffusion boundary such that hybridization will not be hindered by bulk phase diffusion.

Flow experiments

Fluidic chambers were fabricated to investigate the effect of flow on hybridization. Two flow chamber designs with the height of 50 μm and 1 mm were used for investigation of diffusion effect of oligonucleotides. To produce the 50 μm mould, Si wafer was cleaned with RCAI, RCAII and HF and baked on a hotplate at 200 °C for 1 hour to remove moisture contend for better adhesion of photoresist. Subsequently, SU-8 2050, a negative photoresist known for its high Young's modulus, was spin coated at 500 rpm for 2 minutes, and 6000 rpm for 1 minute (see step 2 of Fig.1A). The first spin would create an even distribution of SU-8 on the wafer, and the second spin thin down the SU-8 layer below 10 μm. After spin coating, the layer of photoresist was baked at 65 °C for 3 minutes and 95 °C for 6 minutes and exposed to UV at 365 nm for 30

seconds. The layer serves as an adhesion layer for the structural SU-8 layer that was to be built on top.

The structural layer of SU-8 was spun at 500 rpm for 2 minutes and at 3000 rpm for 1 minute on top of the adhesion layer and prebaked at 65 °C for 3 minutes and 95 °C for 6 minutes to drive out solvent. The prebaked layer was exposed under UV for 90 seconds with a photomask in 15 cycles with 10 seconds interval to avoid overheating and baked again for 1 minute at 65 °C and 5 minutes at 95 °C (step 4 of Fig. 1A). Finally, the SU-8 layer was developed by SU-8 developer for 6 minutes, rinsed in IPA for 2 minutes and cleaned with DI water. The remaining resist image was subjected to hard bake at 150 °C for 30 minutes.

The 1 mm chamber was also produced with a moulding process. The mould for 1mm fluidic chamber was machined from 1mm thick polyethylene terephthalate (PPE) plastic sheet. The mould was then glued onto a clean Si wafer.

After the construction of moulds, the chambers were fabricated with Sylgard 184® Polydimethylsiloxane (PDMS) which offers good chemical and mechanical stability. PDMS was prepared by mixing base and curing agent at 10:1 weight ratio, and then degassed in a vacuum chamber for approximately 1 hour. Poly(methyl methacrylate) (PMMA) frames were arranged around the mould and then brushed with uncured PDMS. The frames were fixed at the location by curing PDMS on a hotplate for 15 minutes. Subsequently the uncured PDMS was then cast into the frames with mould and then degassed for 1 hour. The curing was carried out in a convective oven at 80 °C for 3 hours. Finally, PMMA frames were removed and PDMS chamber was peeled off from Si surface. The chamber was punched to create inlet and outlet, and then plasmaed before pressured on top of the GLAD-MACE wafer to bond with the Si surface reversibly. The entire moulding procedure for the 50 µm microfluidic chambers is shown in Fig. 1A.

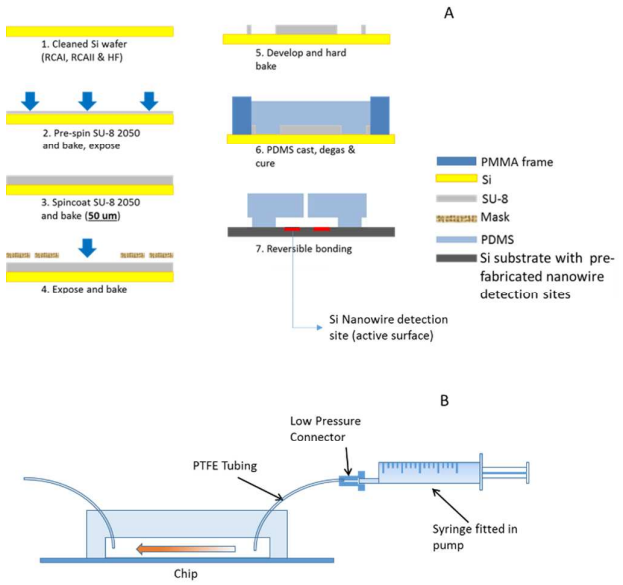

Fig. 1 (A) Fabrication procedure for microfluidic chamber and (B) Fluidic equipment set up.

The microfluidic setup was connected by polytetrafluoroethylene (PTFE) tubings to a KD scientific syringe pump which controls flow rate of analyte solution, as shown schematically in Fig. 1B. Complementary antisense linked with Cy3 was dissolved in PBS with 2% TX-100 at concentration of 1 µM and 0.1 µM. Analyte solution was either pumped through fluidic channel, or dropped directly on top of the functionalized GLAD-MACE substrate (stationary incubation, for comparison). After reaction has proceeded for 1 hour, the hybridization was stopped and substrate was washed 3 times with 2% TX-100 in PBS, followed by DI water wash, and then dried with 100% ethanol. Note that the PDMS chamber bonded on substrate had to be removed first before washing.

3. Results and discussion

Oligonucleotides have commonly been immobilized on solid substrates to serves as probes or to enable surface addressing. On GLAD-MACE substrate, the small size of oligonucleotides probe coupled with 3D surface of nanowires could be a beneficial sensing/microarray platform. We investigated the characteristics of the GLAD-MACE substrate for oligonucleotides immobilization and hybridization.

3.1 Limit of detection and specificity

We first examine the limit of detection (LoD) of GLAD-MACE substrate with hybridization carried out in 1X PBS buffer at room temperature for 2 hours. Oligonucleotide immobilization was performed at 20 µM. The hybridization was performed with the synthetic reference sense-antisense pair, which does not hybridize with naturally occurring oligonucleotide sequence. Such pairs serve as reference for measurement. The sequences of sense (S1) and antisense (AS1) are listed below from 5' to 3':

S1: 5' NH2_C6 AAC AAG CAG AAG GCG GTA GG 3'
AS1:3' TTG TTC GTC TTC CGC CAT CC 5'

The LoD was defined as the lowest concentration to generate a reading higher than background plus 3 times of the standard deviation.

Fig. 2A shows that the GLAD-MACE substrate has an exceptional characteristic for oligonucleotide hybridization. The generated relative fluorescence unit (RFU) with respect to antisense concentration follows a semi log straight line, and the covariance (CV) was always smaller than 10%, making the GLAD-MACE substrate a reliable platform for oligonucleotide quantification. In addition, the lower detection limit was found to be 256 pM with significant differentiation to background (see inset). Coupled with very low hybridization volume (4 µL), such detection limit translate to LoD of 1 fmol (256 pM × 4 µL) or 10^{10} molecules/cm^2. In addition, the resultant detection range spans over 4000 folds from 256 pM to 1000 nM, manifesting an extremely wide dynamic range (DR). In comparison, many oligonucleotide microarrays have dynamic range around 100 fold.[16,17] Note that such limit can be further lowered by using longer incubation time or even higher surface functionalization density. As shown in Fig. 2B, we have functionalized the surface with sense oligonucleotide of 100 µM, and achieved detection limit of 1 pM with overnight incubation of 25 µL of Cy5 labelled antisense, which translates into a LoD of 0.025 fmol.

For microarray, the LoD is critically dependent on a range of factors, such as hybridization buffer composition (cations concentration and species,[18] detergent content,[19] water excluding agent contents[20]), hybridization temperature, hybridization duration, probe sequence and length, antisense sequence and length, detection methods as well as amplification methods. While it is not possible to make exact comparison from results from different groups, we will examine here results obtained from short oligonucleotides hybridization platforms with fluorescent scanning detection method. Alhasan *et al*.[21] used cy5 to label the end of oligonucleotides and they reported on glass slide a detection limit of 10^4 fmol can be achieved with no amplification. Roy *et al*.[22] used Cy3 and FAM to label the oligonucleotides on a flat substrate. They used a microfluidic oscillator to create a turbulent flow to boost hybridization and reported a LoD value of 10 fmol with the set up. The GLAD-MACE substrate produced better LoD as compared to the cited works with no flow oscillation applied. With amplification schemes to boost signal, Liebermann *et al*.[23] used surface plasmonic resonance (SPR) for short oligonucleotides (15mer) detection with fluorophore, and estimated around 10 fold increase of SPR signal from fluorophores compared to the label free detection approach. As a result of amplification, a LoD of 2×10^{10} molecules/cm^2 was achieved. This is similar to the LoD of GLAD-MACE substrate without amplification. Li *et al*. reported a LoD of 0.4 fmol of miRNA on simple flat substrate. The group used alkaline phosphatase for amplification.[24] At sense functionalization concentration of 20 µM, we demonstrated that GLAD-MACE substrate has achieved at least 10 fold lower LoD compared to published results without signal amplification and thus ensure great savings on cost, reagent and reaction time usually associated with the complicated procedures needed for amplification and subsequent washing.

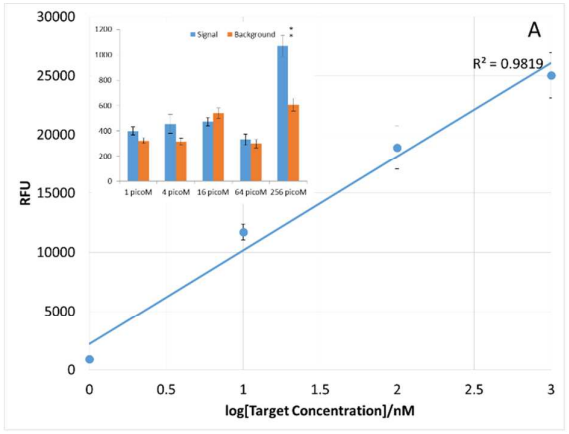

Fig. 2 (A) LoD of GLAD-MACE nanowires functionalized with 20 µM sense for detection of oligonucleotides antisense. Insert: Low concentration conditions. (B) Detection of the same antisense with GLAD-MACE functionalized with 100 µM sense with overnight incubation.

3.2 Specificity for single nucleotide mismatch detection

To investigate the capturing of physiologically relevant oligonucleotides, GLAD-MACE substrate was used to capture hsa-let-7a microRNA (miRNA) mimic. let-7a belongs to let-7 miRNA family found to regulate cell cycles,[25] which can be potentially involved in cancer development[26,27] and involved inflammatory processes.[28] hsa-let-7a is specifically found in human, and the sequence of the capture probe for has-let-7a along with its own sequence are listed below:

Sense: 5' ACT CCA TCA TCC AAC ATA TCA A TTTTTTTTTTTTTTTTTT C6 NH2 3'
Perfect Match (PM) biotin labelled hsa-let-7a miRNA mimic: 3' biotin-UGA GGU AGU AGG UUG UAU AGU U 5'
1 base pair Mismatch (MM) biotin labelled hsa-let-7f miRNA mimic: 3' biotin-UGA GGU AGU AGA UUG UAU AGU U 5'

Let-7a mimic is chemically identical to let-7a, except the biotin labelling at its 3' end. The biotin labelling of miRNA can be achieved with method described by Liang *et al*.[16] and Li *et al*.[24] miRNA can be purified from total RNA sample through miRNA retention column or gel. Briefly, miRNA can be activated with $NaIO_4$ for 90 minutes first and reacted with biotin-x-hydrazide for 3 hours. miRNA can be purified with ethanol preserved in -80^{0}C. The detection is accomplished by hybridization of antisense and probe first, and streptavidin labelled with Cy3 was used to generate signal. hsa-let-7f mimic was included in the hybridization experiment as a measure of discrimination between similar sequences. There is only one nucleotide difference between these two antisense sequences (underlined), representing a challenging scenario for solid surface hybridization due to the interaction of probe and antisense molecules with solid interface. It must be noted the discrimination also varies largely depending on the design of probe,[29] the hybridization environment, the detection method,[30] as well as the location of the single nucleotide difference.

Fig. 3 shows the detection of hsa-let-7a mimic on GLAD-MACE substrate. Like with reference sequences, the detection limit was maintained at fmol level with sense functionalization at 20 µM. We have compared discrimination power at the concentrations of 100 nM of PM antisense and MM antisense and noted a discrimination around 2 fold (see inset of Fig. 3).

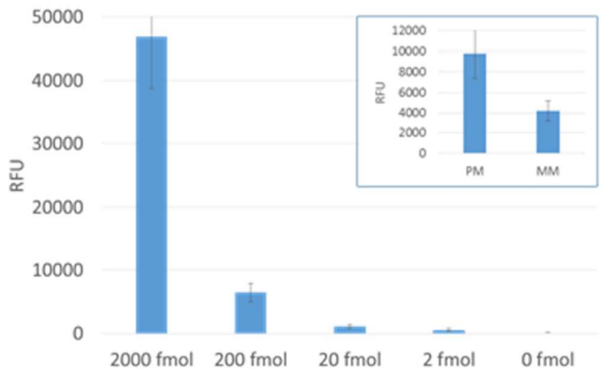

Fig. 3 Detection of hsa-let-7a and single nucleotide discrimination on GLAD-MACE substrate.

This agrees with previous report which[22] showed the single base pair MM has a discrimination ratio around 1.5 fold at 100 nM. According to Fuchs *et al*.,[31] the discrimination measured with SNP oligonucleotides at 37^{0}C without formamide was around 0.9 on biochip surface. According to Oh *et al*.,[32], the discrimination ratio for various surfaces for internal mismatch ranges from 0.2 to 0.6. Our discrimination value corresponds well with literature. In addition, it is possible to improve discrimination with the addition of formamide on GLAD-MACE substrate.[33]

3.3 Factors influencing hybridization

3.3.1 High crosslinking capacity for sense immobilization

Oligonucleotide strand S1-Cy3 was used to examine the loading capacity of the GLAD-MACE nanowires. The 20mer oligonucleotide has GC content of 55% and a molecular weight of 6400 Da; and is considerably larger than the fluorophores (molecular weight around 1000 Da). To gauge the absolute amount of probes immobilized on the surface, probe density was measured at immobilization concentration at 20 µM. Fluorometry was employed to measure the uncrosslinked probes after the reaction to deduct the crosslinked amount. Note that the frequently used in-situ techniques for estimation of surface probe densities such as quartz crystal microbalance,[34] chronocoulometry[6] or surface plasmonic wave sensor[35] are not suitable for GLAD-MACE substrate as quartz crystal microbalance cannot differentiate covalently crosslinked probes to those adsorbed nonspecifically, and the irregular oxide layer on GLAD-MACE nanowires made accurate measurement of charge transfer or plasmonic wave challenging.

Fig. 4A shows the averaged absolute amount of probes crosslinked to GLAD-MACE substrate with a footprint of 2.5mm×2.5mm through a reaction time course of 32 hours. At the end of reaction course of 10 hours, the GLAD-MACE substrate took in around 43 pmol of probes, which translates to a probe density of 4.14×10^{14} probes/cm^2 on the footprint. The probe density is 2 orders of magnitudes higher than most reported values.[36-41] Furthermore, the GLAD-MACE substrate proved to have even higher capacity as the crosslinking signal continues to rise up till 250 µM (shown in Fig. 4B).

We have used porous silica beads to investigate if oligonucleotides can diffuse into pores on GLAD-MACE nanowires. The beads were similarly functionalized, and oligonucleotide conjugation was carried out when beads were stirred in a solution. After reaction, the amount of remaining dye conjugated oligonucleotide was measured to deduce the amount of conjugated oligonucleotides. From our experiments, porous silica beads with 3 nm pores conjugated about 200 times less oligonucleotides as compared to beads with 6 nm pores according to the fluorometry measurement (data not shown). As a result, the porous silica beads with 6 nm pores appeared much redder visibly after reaction, as shown in Fig. 4C. It has been suggested that oligonucleotides were characterized with a very short persistence length,[42] resulting in a small hydrodynamic radius.[43-45] Oligonucleotides with 20-40 bases would likely to have a hydrodynamic radius of 2-3 nm.[46] Our previous thermoporometry measurement[47] indicated that a majority of the pores of our GLAD-MACE nanowires have a pore size of ~6 nm. This is comparable to that on the porous silica particles shown in Fig. 4C. Thus the oligonucleotides could diffuse into the pores on nanowires and contributed to the increased loading capacity on GLAD-MACE substrate.

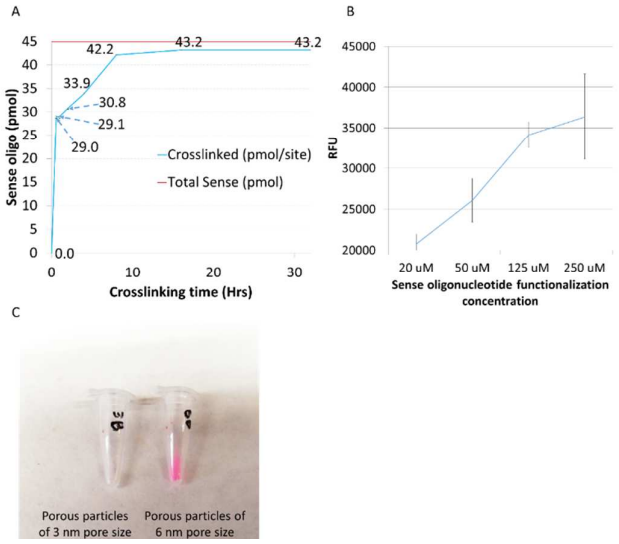

Fig. 4 Crosslinking of oligonucleotides on GLAD-MACE nanowires. (A) Absolute amount of crosslinked probes (B) RFU reading of GLAD-MACE with increasing sense oligonucleotide functionalization concentration and (C) crosslinking of oligonucleotides with beads of different pore sizes.

3.3.2 Low steric hindrance for antisense hybridization

It is often observed that on solid substrate, hybridization efficiency increases first with increasing probe immobilization, but will decrease as probe immobilization continues to rise.[6,48]

The most commonly used substrates for oligonucleotide probes immobilization are silane or gold modified glass or quartz surface.[49] On such substrates, a peak hybridization efficiency for 20 mer was reported at the surface probe density around 1×10^{11} to 4 $\times10^{12}$ probes/cm^2.[6,50,51] Further increase in probe density will lead to excessive steric hindrance and it becomes an obstruction for antisenses to hybridize despite larger hybridization driving force.

The possible steric hindrance effect on GLAD-MACE substrates was investigated by hybridizing equal amount of 1 μM Cy3 linked perfect match antisense sequence to the probe immobilized on the surface. Since antisense concentration is kept constant, the relative strength of RFU represents efficiency of hybridization. Fig. 5 show the hybridization signal change with regard to the probe immobilization concentration. As estimated earlier, the probe density was 4.14×10^{14} probes/cm^2, much larger than typical density of 10^{11} to 10^{12} probes/cm^2 for steric hindrance to occur. The GLAD-MACE substrate demonstrated superior characteristics for hybridization compared to flat substrates in that the hybridization efficiency continued to rise even at the probe immobilization concentration of 20 μM, despite large probe density on GLAD-MACE surface. This is perhaps reasonable as we have estimated[49] that an increase in surface area of 2 orders of magnitudes was obtained in GLAD-MACE substrates.

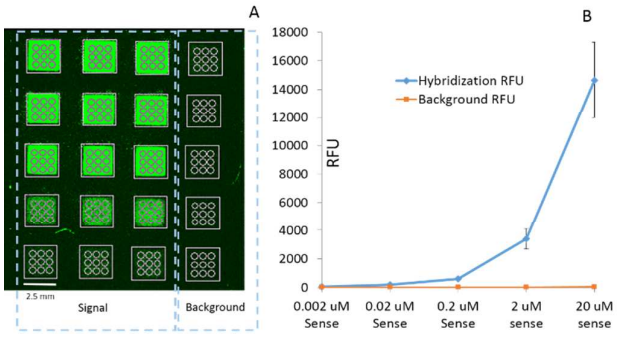

Fig. 5 (A) Scanned image of hybridization signal on sense oligonucleotides functionalized substrates and (B) RFU readings of hybridization.

To quantitatively gauge the effect of steric hindrance, we measured the chemical equilibrium of hybridization. By considering oligonucleotides hybridization reaction where antisenses are in liquid phase and probes are immobilized on solid substrate; the relationship between probes and antisenses can be written as following

$$V[T_o] = V[T] + A[P:T] \quad (1)$$

$$A[T_o] = A[T] + A[P:T] \quad (2)$$

where V is the total reaction volume, $[T]_o$ is original fluorescent antisense concentration in the reaction volume, $[T]$ is the remaining fluorescent antisense concentration. A is the footprint of the probe immobilized surface, $[P]_o$ is the original free probe density, $[P]$ is the remaining free probe density and $[P:T]$ is hybridized probe density on solid surface. According to Stevens *et al.*[52] at equilibrium, the equilibrium dissociation constant Kd can be expressed as

$$\frac{Kd}{[T]_0} = \frac{[F]}{[T]_0}\frac{\frac{A[P]_0}{V[T]_0} - (1-\frac{[T]}{[T]_0})}{(1-\frac{[T]}{[T]_0})} \quad (3)$$

Let

$$s = \frac{A[P]_0}{V[T]_0},\quad k = \frac{Kd}{[T]_0},\quad f = \frac{[T]}{[T]_0}$$

Eq (3) can be re-arranged as

$$f = \frac{-(k+s-1)+\sqrt{(k+s-1)^2+4k}}{2} \quad (4)$$

where

$$k = f\frac{s-(1-f)}{(1-f)} \quad (5)$$

To allow the reaction to reach equilibrium, chaotic flow was created and the reaction was performed for 152 hours. The duration was chosen to ensure maximum hybridization to occur.[52-56] Fig. 6 shows the concentration change of antisense sequence during the reaction course. The measurements fitted well with a first order reaction kinetics (red line). It has been agreed that oligonucleotides hybridization on a flat solid substrate follows pseudo first order reaction when inter-probe repulsion is insignificant.[57-59] The equilibrium constant was determined to be 0.6×10^8 M^{-1} from the remaining oligonucleotide concentration at 152 hour shown in Fig. 6. The value is in good agreement with equilibrium constants reported with flat non-porous substrates[6,35,60,61] or substrates with micro-meter sized features.[52,62] As we have demonstrated, despite accommodating much more oligonucleotides on the surface, the substrate has shown little steric hindrance manifested by the equilibrium constant. Coupled with the high oligonucleotides concentration, it explains the improved performance offered by GLAD-MACE substrate.

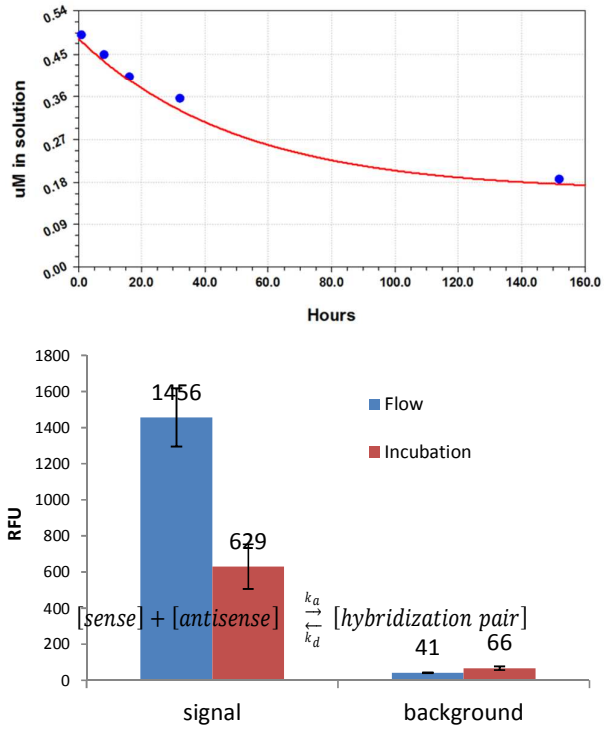

Fig. 6 The concentration change of antisense sequence (remaining antisense concentration in reaction volume) during the reaction course.

3.3.3 Hybridization under flow conditions

So far we have explored the hybridization characteristics of GLAD-MACE substrate under static free incubation. It has been reported oligonucleotides diffusion is a slow process due to their relative large molecule sizes. For oligonucleotides used in our experiment at room temperature, the diffusion constant is close to 9.9×10^{-11} m^2/s;[63] on the other hand, DNA hybridization happens with a very high kinetic association constant around 10^5 $M^{-1}s^{-1}$ between complementary strands, and very low kinetic dissociation constant around 10^{-4}.[63] A simple estimation based on pseudo first order kinetics has a relation as the following:

where k_a is the kinetic association constant, and k_d is kinetic dissociation constant. When there is excessive amount of antisenses in the solution, k_d can be ignored. With our previous results, we found 30 pmol probes can be immobilized after 2 hours on to a detection site with footprint of 2.5 mm×2.5 mm. Assuming the probes are evenly distributed in the detection site with nanowire height of 10 μm, the antisense concentration will change rapidly at a rate of 480 μM/s, and the antisense within 10 μm of the nanowires will be depleted within 0.002 second. Due to the low diffusivity of DNA, the hybridization will soon be a diffusion limited process, where the high speed of DNA hybridization will be masked by the low speed of DNA diffusion.

To counter the depletion problem near nanowires, fluidic chambers were built from PDMS to enable the continuous supply of antisense to GLAD-MACE surface, which could lead to a higher SNR compared to stationary incubation. Stationary incubation was used as a baseline for comparison to gauge the effectiveness of flow. We have demonstrated the deficiency in carrying out fluidic study with a chamber height of 1mm (see Supplementary S1) due to long diffusion distance. According to Pappaert *et al*., the chance of a single molecule colliding with a reactive surface increased dramatically with decreasing bulk liquid layer thickness,[64] as a result, the diffusion characteristic time τ α (H^2/D) also shortens when bulk layer thickness reduces. Thus to speed up diffusion, one simple approach would be to reduce the height of fluidic channel to 50 μm. As shown in Fig.7, in 50 μm chamber, flow hybridization out-performed free incubation with the SNR of 35.5 (1456/41). Repeated experiments showed the SNR of flow hybridization in 50 μm chamber ranges about 3 to 9 times higher than that obtained from free incubation. Further optimization could be achieved by continually shrinking down the height of the chamber as positive effect could be seen with channel height less than 10 μm.

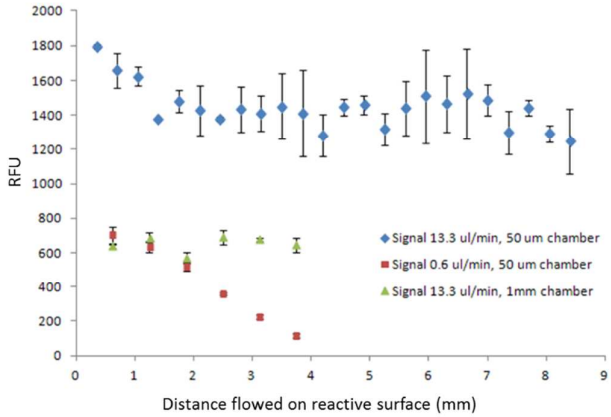

Fig. 7 A comparison of the efficiency of hybridization of a 13.3 μL/min flow in 50 um height microfluidic chamber as compared to stationary incubation.

When transport is the limiting factor, the boundary layer thickness (δ) in a steady state reactor with wall reaction happening only on one side could be approximated[65] to $\delta = (1/0.67)[(DxH)/(3U_m)]^{1/3}$, where x is the distance travelled on reactive surface. Outside the boundary layer, the concentration of the reactants can be regarded as unchanged, inside the boundary layer, reactants are consumed. At steady state, larger δ/H represent a more efficient use of reactants. When chamber height decreased to 50 μm, the mass transport boundary layer extends across chamber height (101 μm from calculation, but maximum is 50 μm) when flow speed is maintained at 26 μm/s (same speed as 1 mm chamber described in supplementary, with flow rate of 0.6 μL/min), or is 37.5 μm when flow rate s maintained (13.6 μL/min), demonstrating better use of oligonucleotides with smaller chamber height.

We performed experiments in the 50 μm chamber with high and low speed flow, and compared the results obtained from 1 mm chamber with results shown in Fig. 8. For high speed flow (13.3 μL/min), 50 μm chamber produced much higher RFU along channel length compared to flow in 1 mm chamber, this is due to much improved efficiency in utilizing antisense. In 50 μm chamber, when flow rate was dropped to 0.6 μL/min to keep the same flow speed as in 1 mm chamber, RFU decreased significantly along channel length; this is due to the limited supply of antisense in 50 μm channel; compared to 1mm channel, in any given time, only 1/20 of reactant was supplied. As such, we have shown that oligonucleotide hybridization on GLAD-MACE is transport limited process. To obtain a uniform response with an improved SNR, microfluidic chamber should be used in conjunction with high flow speed.

Fig. 8 Experiment RFU for fast and slow flow rate for 50 μm chamber, faster flow produced much higher reading (blue dots) compared to slower flow (red dots).

4. Conclusions

In this paper, GLAD-MACE substrate was used as a platform for oligonucleotides hybridization. It is shown that this substrate has large capacity to accommodate a huge amount of probe molecules on the nanowires surface and pores on the sidewall, thus could be used to increase the limit of detection as oligonucleotide microarray. In contrast to conventional substrate, Au GLAD-MACE nanowires can accept 100 times more probes without showing probe steric hindrance. Compared to detection of oligonucleotides with fluorescent reporters on a traditional substrate, even those with the facilitate of microfluidic mixing chamber, at least a 10 times lower LoD can be reached with a passive hybridization strategy. The enhanced sensitivity mainly comes from increased loading capacity, as we have not observed significant difference of chemical equilibrium from reported literatures.

For device built with GLAD-MACE nanowires, it is clear that one important factor to optimize the system performance is to design an apparatus that can speed up the diffusion process of antisenses. We have shown with our microfluidics set up, the signal read out from GLAD-MACE increased 3 to 9 fold. It is important to further optimize the fluidic set up so that a miniaturized user friendly device should be explored.

Acknowledgements

This work was supported by a Proof-of-Concept grant (POC R-263-000-A11-281) by the National Research Foundation (Singapore). HC, JXW and HZ would like to thank the Singapore-MIT Alliance, NUS Graduate School for Integrative Sciences and Engineering and GLOBALFOUNDARIES Singapore Pte. Ltd. for the providing scholarships. WX would like to acknowledge the Department of Electrical and Computer Engineering for the provision of a research assistantship.

References

1. Y. J. Hua, K. Tu, K. Z. Y. Tang, Y. X. Li and H. S. Xiao, *Genomics,* 2008, **92**, 122-128.
2. Y. Rao, Y. Lee, D. Jarjoura, A. S. Ruppert, C. G. Liu, J. C. Hsu and J. P. Hagan, *Statistical Applications in Genetics and Molecular Biology,* 2008, **7**, 22.
3. M. F. Templin, D. Stoll, D. M. Schrenk, P. C. Traub, C. F. Vöhringer and T. O. Joos, *Trends in Biotechnol.,* 2002, **20**, 160-166.
4. D. S. Wilson and S. Nock, *Angew. Chem., Int. Ed.,* 2003, **42**, 494-500.
5. H. Zhu and M. Snyder, *Curr. Opin. Chem. Biol.,* 2003, **7**, 55-63.
6. A. B. Steel, T. M. Herne and M. J. Tarlov, *Anal. Chem.,* 1998, **70**, 4670-4677.
7. B. J. Hong, V. Sunkara and J. W. Park, *Nucleic Acids Res.,* 2005, **33**, e106-1-e106-8.
8. P. K. Ajikumar, J. K. Ng, Y. C. Tang, J. Y. Lee, G. Stephanopoulos and H. P. Too, *Langmuir,* 2007, **23**, 5670-5677.
9. R. S. Foote, J. Khandurina, S. C. Jacobson, and J. M. Ramsey, *Anal. Chem.,* 2005, **77**, 57-63.
10. J. Drott, K. Lindström, L. Rosengren and T. Laurell, *J. Micromechanics and Microengineering* 1997, **7**, 14-23.
11. B. R. Murthy, J. K. K. Ng, E. S. Selamat, N. Balasubramanian and W. T. Liu, *Biosens. Bioelectron.,* 2008, **24**, 723-728.
12. S. Gautsch and H. F. De Rooij, *Microelectron. Engineering,* 2011, **88**, 2533-2536.
13. K. Tsougeni, G. Koukouvinos, P. S. Petrou, A. Tserepi, S. E. Kakabakos and E. Gogolides, *Anal. Bioanal. Chem.,* 2012, **403**, 2757-2764.
14. M. K. Dawood, L. Zhou, H. Zheng, H. Cheng, G. Wan, R. Rajagopalan, H. P. Too and W. K. Choi, *Lab on a Chip,* 2012, **12**, 5016-5024.
15. P. Buchegger, U. Sauer, H. Toth-Székély and C. Preininger, *Sensors,* 2012, **12**, 1494-1508.
16. R. Q. Liang, W. Li, Y. Li, C. Y. Tan, J. X. Li, Y. X. Jin and K. C. Ruan, *Nucleic Acids Res.,* 2005, **33**, e17-1-e17-8.
17. B. Zhao, S. Ding, W. Li and Y. Jin, *Acta Biochimica et Biophysica Sinica,* 2011, **43**, 551-555.
18. T. Špringer, H. Šípová, H. Vaisocherová, J. Štepánek and J. Homola, *Nucleic Acids Res.,* 2010, **38**, 7343-7351.
19. M. Sastry, A. Kumar, M. Pattarkine, V. Ramakrishnan and K. N. Ganesh, *Chem. Commun.,* 2001, **16**, 1434-1435.
20. N. Dave and J. Liu, *J. Phys. Chem. B,* 2010, **114**, 15694-15699.
21. A. H. Alhasan, D. Y. Kim, W. L. Daniel, E. Watson, J. J. Meeks, C. S. Thaxton and C. A. Mirkin, *Anal. Chem.,* 2012, **84**, 4153-4160.
22. S. Roy, J. H. Soh, and Z. Gao, *Lab on a Chip,* 2011, **11**, 1886-1894.
23. T. Liebermann, W. Knoll, P. Sluka and R. Herrmann, *Colloids and Surfaces A,* 2000, **169**, 337-350.
24. W. Li, B. Zhao, Y. Jin and K. Ruan, Acta *Biochimica et Biophysica Sinica,* 2010, **42**, 296-301.
25. C. D. Johnson, A. Esquela-Kerscher, G. Stefani, M. Byrom, K. Kelnar, D. Ovcharenko, M. Wilson, X. Wang, J. Shelton, J. Shingara, L. Chin, D. Brown and F. J. Slack, *Cancer Res.,* 2007, **67**, 7713-7722.
26. S. M. Johnson, H. Grosshans, J. Shingara, M. Byrom, R. Jarvis, A. Cheng, E. Labourier, K. L. Reinert, D. Brown and F. J. Slack, *Cell,* 2005, **120**, 635-647.

27. S. Shell, S. M. Park, A. R. Radjabi, R. Schickel, E. O. Kistner, D. A. Jewell, C. Feig, E. Lengyel and M. E. Peter, *Proc. Natl. Acad. Sci. USA,* 2007, **104**, 11400-11405.
28. M. Kumar, T. Ahmad, A. Sharma, U. Mabalirajan, A. Kulshreshtha, A. Agrawal and B. Ghosh, *J. Allergy and Clinical Immunology,* 2011, **128**, 1077-1085.
29. S. N. Gardner, J. B. Thissen, K. S. McLoughlin, T. Slezak and C. J. Jaing, *J. Microbiological Methods,* 2013, **94**, 303-310.
30. H. Miyachi, K. Ikebukuro, K. Yano, H. Aburatani and I. Karube, *Biosens. Bioelectron.* 2004, **20**, 184-189.
31. J. Fuchs, D. Dell'Atti, A. Buhot, R. Calemczuk, M. Mascini and T. Livache, *Anal. Biochem.,* 2010, **397**, 132-134.
32. S. J. Oh, S. J. Cho, C. O. Kim and J. W. Park, *Langmuir,* 2002, **18**, 1764-1769.
33. H. Cheng, H. Zheng, J. X. Wu, W. Xu, L. Zhou, K. C. Leong, E.A. Fitzgerald, R. Rajagopalan, H. P. Too and W. K. Choi, *PLoS One,* 2015, **10**, e0116539-1-e0116539-16.
34. Y. K. Cho, S. Kim, Y. A. Kim, H. K. Lim, K. Lee, D. Yoon, G. Lim, Y. E. Pak, T. H. Ha and K. Kim, *J. Colloid and Interface Sci.,* 2004, **278**, 44-52.
35. F. Yu, D. Yao and W. Knoll, *Nucleic Acids Res.,* 2004, **32**, e75-1-e75-7.
36. M. D. Kane, T. A. Jatkoe, C. R. Stumpf, J. Lu, J. D. Thomas and S. J. Madore, *Nucleic Acids Res.,* 2000, **28**, 4552-4557.
37. J. B. Lamture, K. L. Beattie, B. E. Burke, M. D. Eggers, D. J. Ehrlich, R. Fowler, M. A. Hollis, B. B. Kosicki, R. K. Reich, S. R. Smith, R. S. Varma and M. E. Hogan, *Nucleic Acids Res.,* 1994, **22**, 2121-2125.
38. L. M. Smith, *Anal. Chem.* 1997, **69**, 4948-4956.
39. T. Strother, W. Cai, X. Zhao, R. J. Hamers and L. M. Smith, *J. Am. Chem. Soc.,* 2000, 122,1205-1209.
40. T. Strother, R. J. Hamers and L. M. Smith, *Nucleic Acids Res.,* 2000, **28**, 3535-3541.
41. J. Wang, *Nucleic Acids Res.,* 2000, **28**, 3011-3016.
42. M. X. Fernandes, A. Ortega, M. C. López Martínez and J. García de la Torre, *Nucleic Acids Res.,* 2002, **30**, 1782-1788.
43. S. Geggier, A. Kotlyar and A. Vologodskii, *Nucleic Acids Res.,* 2011, **39**, 1419-1426.
44. H. Chen, S. P. Meisburger, S. A. Pabit, J. L. Sutton, W. W. Webb and L. Pollack, *Proc. Natl. Acad. Sci. USA,* 2012, **109**, 799-804.
45. Q. Chi, G. Wang and J. Jiang, *Physica A,* 2013, 392, 1072-1079.
46. A. Y. L. Sim, J. Lipfert, D. Herschlag and S. Doniach, *Phys. Rev. E,* 2012, **86**, 021901-1-021901-5.
47. J. X. Wu, H. Zheng, H. Cheng, L. Zhou, K. C. Leong, R. Rajagopalan, H. P. Too and W. K. Choi, *Langmuir,* 2014, **30**, 2206-2215.
48. R. Levicky and A. Horgan, *Trends in Biotechnol.,* 2005, **23**, 143-149.
49. M. C. Pirrung, *Angew. Chem., Int. Ed.,* 2002, **41**, 1276-1289.
50. J. H. Watterson, P. A. E. Piunno, C. C. Wust and U. J. Krull, *Langmuir,* 2000, **16**, 4984-4992.
51. J. H. Watterson, P. A. E. Piunno and U. J. Krull, *Anal. Chim. Acta,* 2002, **457**, 29-38.
52. P. W. Stevens, M. R. Henry and D. M. Kelso, *Nucleic Acids Res.,* 1999, **27**, 1719-1727.
53. M. R. Henry, P. Wilkins Stevens, J. Sun and D. M. Kelso, *Anal. Biochem.,* 1999, **276**, 204-214.
54. W. Michel, T. Mai, T. Naiser and A. Ott, *Biophys Journal,* 2007, **92**, 999-1004.
55. D. J. Fish, M. T. Horne, G. P. Brewood, J. P. Goodarzi, S. Alemayehu, A. Bhandiwad, R. P. Searles and A. S. Benight, *Nucleic Acids Res.,* 2007, **35**, 7197-7208.
56. M. Glazer, J. Fidanza, G. McGall and C. Frank, *Chem. Mater.,* 2001, **13**, 4773-4782.
57. H. Su and M. Thompson, *Biosens. Bioelectron.,*1995, **10**, 329-340.
58. D. Yao, J. Kim, F. Yu, P. E. Nielsen, E. K. Sinner and W. Knoll, *Biophys. Journal,* 2005, **88**, 2745-2751.
59. M. Lazerges, H. Perrot, N. Rabehagasoa, C. Compère, C. Dreanno, M. Mucio Pedroso, R. C. Faria and P. R. Bueno, *Sensors and Actuators B,* 2012, **171-172**, 522-527.
60. A. W. Peterson, L. K. Wolf, and R. M. Georgiadis, *J. Am. Chem. Soc.,* 2002, **124**, 14601-14607.
61. Y. Okahata, M. Kawase, K. Niikura, F. Ohtake, H. Furusawa and Y. Ebara, *Anal. Chem.,* 1998, **70**, 1288-1291.
62. M. Glazer, J. A. Fidanza, G. H. McGall, M. O. Trulson, J. E. Forman, A. Suseno and C. W. Frank, *Anal. Biochem.,* 2006, **358**, 225-238.
63. Y. Gao, L. K. Wolf and R. M. Georgiadis, *Nucleic Acids Res.,* 2006, **34**, 3370-3377.
64. K. Pappaert, P. Van Hummelen, J. Vanderhoeven, G. V. Baron and G. Desmet, *Chem. Engineering Sci.,* 2003, **58**, 4921-4930.
65. J. H. S. Kim, A. Marafie, X. Y. Jia, J. V. Zoval and M. J. Madou, *Sensors and Actuators B,* 2006, **113**, 281-289.

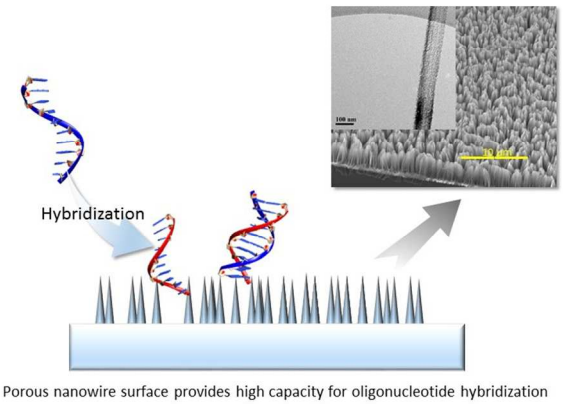

Porous nanowire surface provides high capacity for oligonucleotide hybridization

338x190mm (96 x 96 DPI)